

Supplement of Atmos. Chem. Phys., 18, 11647–11661, 2018  
<https://doi.org/10.5194/acp-18-11647-2018-supplement>  
© Author(s) 2018. This work is distributed under  
the Creative Commons Attribution 4.0 License.



Atmospheric  
Chemistry  
and Physics  
Open Access  
EGU

*Supplement of*

## **Nitrogen isotope fractionation during gas-to-particle conversion of $\text{NO}_x$ to $\text{NO}_3^-$ in the atmosphere – implications for isotope-based $\text{NO}_x$ source apportionment**

**Yunhua Chang et al.**

*Correspondence to:* Yanlin Zhang ([dryanlinzhang@outlook.com](mailto:dryanlinzhang@outlook.com), [dryanlinzhang@nuist.edu.cn](mailto:dryanlinzhang@nuist.edu.cn))

The copyright of individual parts of the supplement might differ from the CC BY 4.0 License.

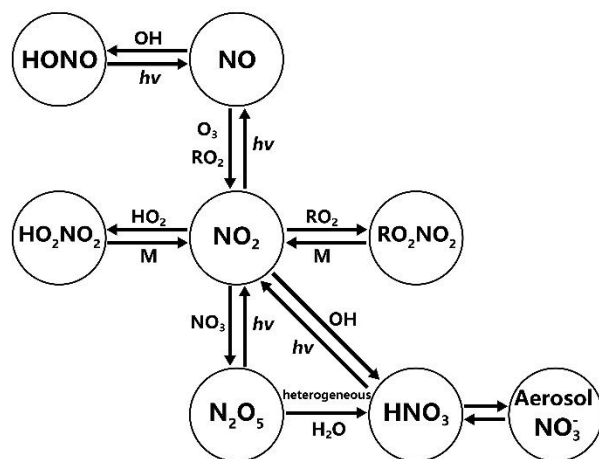


**Figure S1.** Possible NO<sub>x</sub> to NO<sub>3</sub><sup>-</sup> transformation pathways

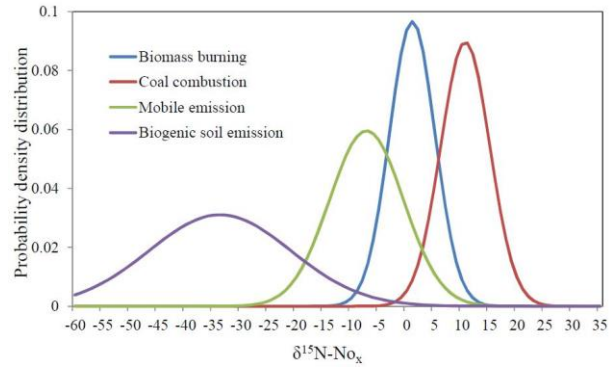


**Figure S2.** Probability density distribution of  $\delta^{15}\text{N-NO}_x$  emitted from the four  $\text{NO}_x$  sources considered in this study.

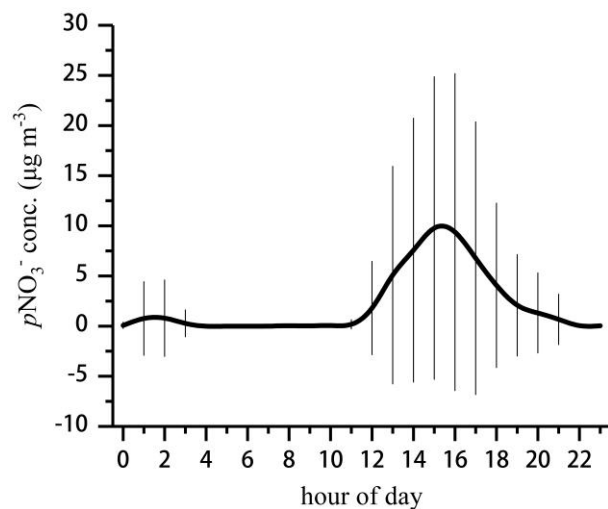


**Figure S3.** Diurnal variation of the mass concentration (mean  $\pm 1\sigma$ ) of nitrate formed through  $\bullet\text{OH}$  oxidation of  $\text{NO}_2$  in Nanjing City.

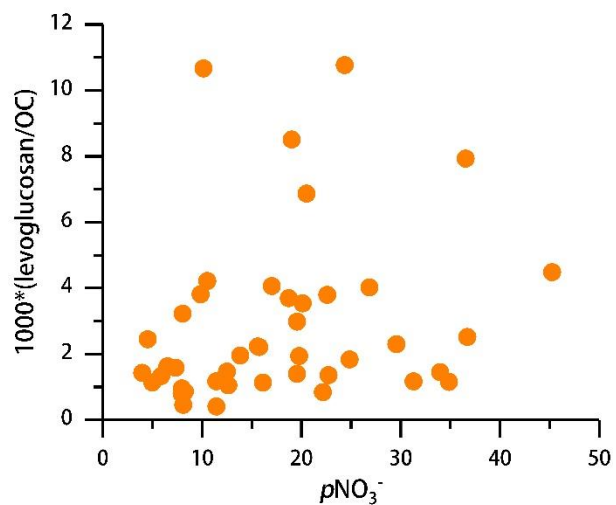


**Figure S4.** Scatter plot between the mass concentrations of  $pNO_3^-$  ( $\mu\text{g m}^{-3}$ ) and  $1000*(levoglucosan/OC)$  during the Nanjing sampling campaign. The absence of any significant correlation indicates that biomass-burning can be excluded as major  $pNO_3^-$  source.

**Table S1.** Values for the coefficients A, B, C, D used for the calculation of  $^{15}\alpha_{\text{NO}_2/\text{NO}}$ ,  $^{15}\alpha_{\text{N}_2\text{O}_5/\text{NO}_2}$ ,  $^{18}\alpha_{\text{NO}_2/\text{NO}}$ , and  $^{18}\alpha_{\text{OH}/\text{H}_2\text{O}}$  over the settled temperature range (150-450 K) (see main text).

$^{m}\alpha_{XY}$	A	B	C	D	equation
$^{15}\text{NO}_2/\text{NO}$	3.8834	-7.7299	6.0101	-0.17928	2
$^{15}\text{N}_2\text{O}_5/\text{NO}_2$	0.69398	-1.9859	2.3876	0.16308	3
$^{18}\text{NO}/\text{NO}_2$	-0.04129	1.1605	-1.8829	0.74723	5
$^{18}\text{H}_2\text{O}/\text{OH}$	2.1137	-3.8026	2.5653	0.59410	5

**Table S2.** Typical  $\delta^{15}\text{N-NO}_x$  from coal combustion, mobile source and biomass burning based on literature values.

Source types	Mean	Standard deviation	Statistic number	Distribution	Reference
Coal combustion	13.72	4.57	47	Figure S2	1-3
Mobile source	-7.25	7.80	151	Figure S2	3-6
Biomass burning	1.04	4.13	24	Figure S2	7-9
Biogenic soil emission	-33.77	12.16	6	Figure S2	2, 7

**Table S3.** Sample information for Sanjiang sampling campaign

Sample ID	Day/Night	Start (local time)	End (local time)
1	Day	2013/10/8 10:20	2013/10/8 16:20
2	Night	2013/10/8 16:00	2013/10/9 06:00
3	Night	2013/10/9 19:35	2013/10/10 07:35
4	Day	2013/10/10 08:30	2013/10/10 15:30
5	Night	2013/10/10 15:51	2013/10/11 05:51
6	Day	2013/10/11 08:15	2013/10/11 15:45
7	Night	2013/10/17 16:24	2013/10/18 06:24
8	Day	2013/10/18 08:59	2013/10/18 15:59



**Table S4.** Site information and descriptive statistics for  $\delta^{15}\text{N}$  values for atmospheric  $\text{NO}_3^-$  extracted from the literature.

Site name	Type	Phase	N	Mean	SD	Minimum	Median	Maximum	Reference
Yongxing Island	marine	aerosol	53	1.19	1.65	-2.45	1.36	4.88	11
Mt. Lulin	background	aerosol	174	-3.50	3.74	-17.21	-3.05	6.50	12
Jeju Island	marine	aerosol	81	3.81	2.51	0.59	3.28	15.33	13
Dongsha Island	marine	rainwater	18	-4.86	1.40	-7.51	-5.03	-1.77	14
Botanical Garden	background	rainwater	105	3.70	2.48	-4.90	3.88	10.35	15
Beihuang Island	marine	rainwater	120	8.20	6.18	-1.72	5.95	23.98	16
experimental field	suburban	rainwater	30	1.62	2.99	-3.24	1.24	7.25	17
Dongbeiwang	suburban	rainwater	21	6.82	5.78	-1.88	6.40	20.94	17
Changping	rural	rainwater	28	2.53	5.48	-3.80	1.30	20.81	17
Quzhou	rural	rainwater	24	-1.40	3.77	-8.33	-0.20	4.07	17
Wuqiao	rural	rainwater	24	-1.05	3.81	-7.49	-1.71	6.41	17
Wanzhou	rural	rainwater	12	0.23	8.07	-6.46	-3.13	21.92	18
Dade	rural	rainwater	10	-0.65	9.57	-6.88	-3.75	25.00	18

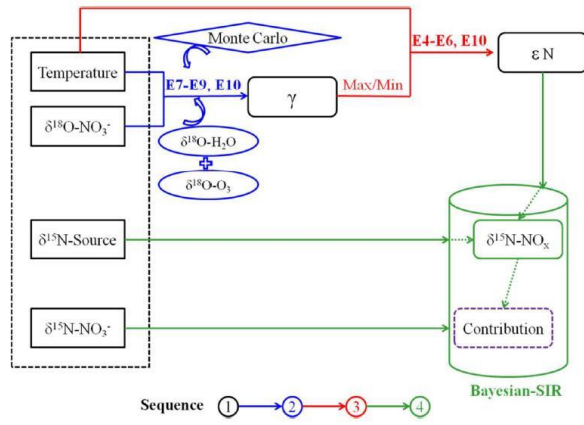
11. Xiao, H.-W.; Xie, L.-H.; Long, A.-M.; Ye, F.; Pan, Y.-P.; Li, D.-N.; Long, Z.-H.; Chen, L.; Xiao, H.-Y.; Liu, C.-Q., Use of isotopic compositions of nitrate in TSP to identify sources and chemistry in South China Sea. *Atmos. Environ.* **2015**, *109*, (Supplement C), 70-78.
12. Guha, T.; Lin, C. T.; Bhattacharya, S. K.; Mahajan, A. S.; Ou-Yang, C.-F.; Lan, Y.-P.; Hsu, S. C.; Liang, M.-C., Isotopic ratios of nitrate in aerosol samples from Mt. Lulin, a high-altitude station in Central Taiwan. *Atmos. Environ.* **2017**, *154*, (Supplement C), 53-69.
13. Kundu, S.; Kawamura, K.; Lee, M., Seasonal variation of the concentrations of nitrogenous species and their nitrogen isotopic ratios in aerosols at Gosan, Jeju Island: Implications for atmospheric processing and source changes of aerosols. *J. Geophys. R.* **2010**, *115*, (D20), DOI: 10.1029/2009JD013323.
14. Yang, J. Y. T.; Hsu, S. C.; Dai, M. H.; Hsiao, S. S. Y.; Kao, S. J., Isotopic composition of water-soluble nitrate in bulk atmospheric deposition at Dongsha Island: sources and implications of external N supply to the northern South China Sea. *Biogeosci.* **2014**, *11*, (7), 1833-1846.
15. Fang, Y. T.; Koba, K.; Wang, X. M.; Wen, D. Z.; Li, J.; Takebayashi, Y.; Liu, X. Y.; Yoh, M., Anthropogenic imprints on nitrogen and oxygen isotopic composition of precipitation nitrate in a nitrogen-polluted city in southern China. *Atmos. Chem. Phys.* **2011**, *11*, (3), 1313-1325.
16. Zong, Z.; Wang, X.; Tian, C.; Chen, Y.; Fang, Y.; Zhang, F.; Li, C.; Sun, J.; Li, J.; Zhang, G., First assessment of  $\text{NO}_x$  sources at a regional background site in North China using isotopic analysis linked with modeling. *Environ. Sci. Technol.* **2017**, *51*, (11), 5923-5931.
17. Zhang, Y.; Liu, X. J.; Fangmeier, A.; Goulding, K. T. W.; Zhang, F. S., Nitrogen inputs and isotopes in precipitation in the North China Plain. *Atmos. Environ.* **2008**, *42*, (7), 1436-1448.
18. Leng, Q.; Cui, J.; Zhou, F.; Du, K.; Zhang, L.; Fu, C.; Liu, Y.; Wang, H.; Shi, G.; Gao, M.; Yang, F.; He, D., Wet-only deposition of atmospheric inorganic nitrogen and associated isotopic characteristics in a typical mountain area, southwestern China. *Sci. Total Environ.* **2018**, *616-617*, (Supplement C), 55-63.

## **Text S1.**

The Bayesian mixing model makes use of stable isotope data to determine the probability distribution of source contributions to a mixture, explicitly accounting for uncertainties associated with multiple sources, their isotopic signatures, and isotope fractionation during transformations.<sup>26</sup> The model has been widely used in ecological studies, such as food-web analyses.<sup>27</sup> In Bayesian theorem, the contribution of each source is calculated based on mixed data and prior information, such that:

$$P(f_q | \text{data}) = \theta(\text{data} | f_q) \times p(f_q) / \sum \theta(\text{data} | f_q) \times p(f_q)$$

where  $\theta(\text{data}|f_q)$  and  $p(f_q)$  refer to the likelihood of the given mixed isotope signature, and the pre-determined probability of the given state of nature, based on prior information, respectively. The denominator represents the numerical approximation of the marginal probability of the data. In a Bayesian model (stable isotope mixing models using sampling-importance-resampling; MixSIR), isotope signatures from the mixed data pool are assumed to be normally distributed. Uncertainty in the distribution of isotope sources and their associated fractionation are factored into the model by defining respective mean ( $\mu$ ) and standard deviation ( $\sigma$ ) parameters. Prior knowledge about proportional source contributions ( $f_q$ ) are defined using the Dirichlet distribution, with an interval of [0, 1]. To assess the likelihood of the given  $f_q$ , the proposed proportional contribution is combined with a user-specified isotope distribution of sources and their associated isotope effects to develop a proposed isotope distribution for the mixture. The posterior probability of proportional source contributions ( $f_q$ ) is calculated by the Hilborn sampling-importance-resampling method. For the detailed model frame and computing method, readers should refer to Moore et al.<sup>28</sup> Based on work by Walters and Michalski,<sup>29</sup> a computation module evaluating the fractionation of the equilibrium/Leighton reaction was incorporated into MixSIR (Figure below and main text).



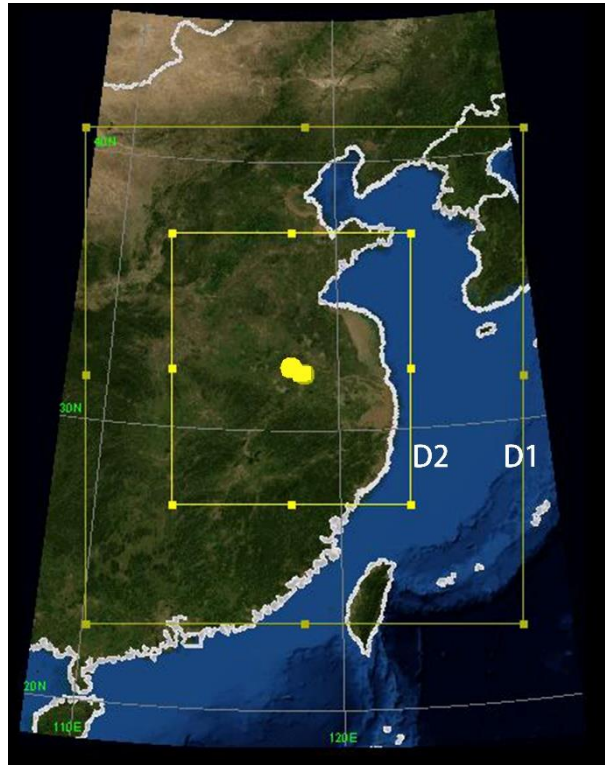
Principle of the Bayesian model approach used in this study.

**Text S2.**

As potential NO<sub>x</sub> sources from emission inventories, coal combustion, mobile source, biomass burning and biogenic soil emissions were considered the dominant contributors to NO<sub>x</sub> in this study (see discussion in the main text). The mean and standard deviations (SD) of  $\delta^{15}\text{N-NO}_x$  for the four type sources (Fig. S2) were calculated based on data from the literature (see Table S2). In this study, the  $\delta^{15}\text{N-NO}_x$  range of vehicle exhaust is considered representative of automotive NO<sub>x</sub> sources in general.

### **Text S3.**

The WRF-Chem (Weather Research and Forecasting model coupled with Chemistry) model v3.6.1<sup>19</sup> was used for simulating the contribution of the two major pathways to form nitrate: NO<sub>2</sub> oxidation by OH and O<sub>3</sub>, respectively. The simulation was adopted from a mother domain with a 27 × 27 km horizontal resolution over eastern China, and nested down to a second domain of 9 × 9 km covering the Yangtze River Delta region. Lambert conformal conic projection was used with true latitude limits of 30.0°N and 60.0°N and standing longitude of 118.0°E. The coverage of the two-way nested domains is shown below. The number of vertical grids used was 30, and the number of horizontal grids was 66 × 75 and 109 × 124, respectively. For formulation of the tropospheric gas and aerosol chemistry (“mechanism”) the gas-phase chemical mechanism CBMZ<sup>20</sup> was used, coupled with the 4-bin sectional MOSAIC model with aqueous chemistry.<sup>21</sup> MOSAIC integrates all the important aerosol species, including sulfate, nitrate, chloride, ammonium, sodium, black carbon, primary organic mass, liquid water and other inorganic mass.<sup>21</sup> Other physical parameterization options include Morrison 2-moment<sup>22</sup>, RRTMG short and long wave radiation,<sup>23</sup> Noah land surface model, and the Yonsei University planetary boundary layer parameterization<sup>24</sup>. Data from the National Center for Environmental Prediction (NCEP) Final (FNL) Operational Global Analysis data set (<http://rda.ucar.edu/datasets/ds083.2/>) with a horizontal resolution of 1°×1° were incorporated as initial and boundary conditions for the model. The chemical initial and boundary conditions are provided by The Model for Ozone and Related chemical Tracers, version 4 (MOZART-4).<sup>25</sup>



Two-way nested modeling domains at 27-km (East Asia: D1), 9-km (Yangtze River Delta: D2) resolutions. Yellow circle represents the observation site in Nanjing City

## Reference

19. Felix, J. D.; Elliott, E. M.; Avery, G. B.; Kieber, R. J.; Mead, R. N.; Willey, J. D.; Mullaugh, K. M., Isotopic composition of nitrate in sequential Hurricane Irene precipitation samples: Implications for changing NO<sub>x</sub> sources. *Atmos. Environ.* **2015**, *106*, 191-195.
20. Felix, J. D.; Elliott, E. M.; Shaw, S. L., Nitrogen isotopic composition of coal-fired power plant NO<sub>x</sub>: influence of emission controls and implications for global emission inventories. *Environ. Sci. Technol.* **2012**, *46*, (6), 3528-3535.
21. Walters, W. W.; Tharp, B. D.; Fang, H.; Kozak, B. J.; Michalski, G., Nitrogen isotope composition of thermally produced NO<sub>x</sub> from various fossil-fuel combustion sources. *Environ. Sci. Technol.* **2015**, *49*, (19), 11363-11371.
22. Felix, J. D.; Elliott, E. M., Isotopic composition of passively collected nitrogen dioxide emissions: Vehicle, soil and livestock source signatures. *Atmos. Environ.* **2014**, *92*, 359-366.
23. Heaton, T. H. E.; Spiro, B.; Madeline, S.; Robertson, C., Potential canopy influences on the isotopic composition of nitrogen and sulphur in atmospheric deposition. *Oecologia* **1997**, *109*, (4), 600-607.
24. Walters, W. W.; Goodwin, S. R.; Michalski, G., Nitrogen stable isotope composition ( $\delta^{15}\text{N}$ ) of vehicle-emitted NO<sub>x</sub>. *Environ. Sci. Technol.* **2015**, *49*, (4), 2278-2285.
25. Fibiger, D. L.; Hastings, M. G., First measurements of the nitrogen isotopic composition of NO<sub>x</sub> from biomass burning. *Environ. Sci. Technol.* **2016**, *50*, (21), 11569-11574.
26. Felix, J. D.; Elliott, E. M., The agricultural history of human-nitrogen interactions as recorded in ice core  $\delta^{15}\text{N-NO}_3^-$ . *Geophys. Res. Lett.* **2013**, *40*, (8), 1642-1646.
27. Hastings, M. G.; Jarvis, J. C.; Steig, E. J., Anthropogenic impacts on nitrogen isotopes of ice-core nitrate. *Science* **2009**, *324*, (5932), 1288-1288.
28. Li, D.; Wang, X., Nitrogen isotopic signature of soil-released nitric oxide (NO) after fertilizer application. *Atmos. Environ.* **2008**, *42*, (19), 4747-4754.
29. Xiao, H.-W.; Xie, L.-H.; Long, A.-M.; Ye, F.; Pan, Y.-P.; Li, D.-N.; Long, Z.-H.; Chen, L.; Xiao, H.-Y.; Liu, C.-Q., Use of isotopic compositions of nitrate in TSP to identify sources and chemistry in South China Sea. *Atmos. Environ.* **2015**, *109*, (Supplement C), 70-78.
30. Guha, T.; Lin, C. T.; Bhattacharya, S. K.; Mahajan, A. S.; Ou-Yang, C.-F.; Lan, Y.-P.; Hsu, S. C.; Liang, M.-C., Isotopic ratios of nitrate in aerosol samples from Mt. Lulin, a high-altitude station in Central Taiwan. *Atmos. Environ.* **2017**, *154*, (Supplement C), 53-69.
31. Kundu, S.; Kawamura, K.; Lee, M., Seasonal variation of the concentrations of nitrogenous species and their nitrogen isotopic ratios in aerosols at Gosan, Jeju Island: Implications for atmospheric processing and source changes of aerosols. *J. Geophys. R.* **2010**, *115*, (D20), DOI: 10.1029/2009JD013323.
32. Yang, J. Y. T.; Hsu, S. C.; Dai, M. H.; Hsiao, S. S. Y.; Kao, S. J., Isotopic composition of water-soluble nitrate in bulk atmospheric deposition at Dongsha Island: sources and implications of external N supply to the northern South China Sea. *Biogeosci.* **2014**, *11*, (7), 1833-1846.

33. Fang, Y. T.; Koba, K.; Wang, X. M.; Wen, D. Z.; Li, J.; Takebayashi, Y.; Liu, X. Y.; Yoh, M., Anthropogenic imprints on nitrogen and oxygen isotopic composition of precipitation nitrate in a nitrogen-polluted city in southern China. *Atmos. Chem. Phys.* **2011**, *11*, (3), 1313-1325.
34. Zong, Z.; Wang, X.; Tian, C.; Chen, Y.; Fang, Y.; Zhang, F.; Li, C.; Sun, J.; Li, J.; Zhang, G., First assessment of NO<sub>x</sub> sources at a regional background site in North China using isotopic analysis linked with modeling. *Environ. Sci. Technol.* **2017**, *51*, (11), 5923-5931.
35. Zhang, Y.; Liu, X. J.; Fangmeier, A.; Goulding, K. T. W.; Zhang, F. S., Nitrogen inputs and isotopes in precipitation in the North China Plain. *Atmos. Environ.* **2008**, *42*, (7), 1436-1448.
36. Leng, Q.; Cui, J.; Zhou, F.; Du, K.; Zhang, L.; Fu, C.; Liu, Y.; Wang, H.; Shi, G.; Gao, M.; Yang, F.; He, D., Wet-only deposition of atmospheric inorganic nitrogen and associated isotopic characteristics in a typical mountain area, southwestern China. *Sci. Total Environ.* **2018**, *616-617*, (Supplement C), 55-63.
37. Grell, G. A.; Peckham, S. E.; Schmitz, R.; McKeen, S. A.; Frost, G.; Skamarock, W. C.; Eder, B., Fully coupled “online” chemistry within the WRF model. *Atmos. Environ.* **2005**, *39*, (37), 6957-6975.
38. Zaveri, R. A.; Peters, L. K., A new lumped structure photochemical mechanism for large-scale applications. *J. Geophys. Res.* **1999**, *104*, (D23), 30387-30415.
39. Zaveri, R. A.; Easter, R. C.; Fast, J. D.; Peters, L. K., Model for Simulating Aerosol Interactions and Chemistry (MOSAIC). *J. Geophys. Res.* **2008**, *113*, (D13), DOI: 10.1029/2007JD008782.
40. Morrison, H.; Thompson, G.; Tatarskii, V., Impact of cloud microphysics on the development of trailing stratiform precipitation in a simulated squall line: Comparison of one- and two-moment schemes. *Mon. Wea. Rev.* **2009**, *137*, (3), 991-1007.
41. Iacono, M. J.; Mlawer, E. J.; Clough, S. A.; Morcrette, J.-J., Impact of an improved longwave radiation model, RRTM, on the energy budget and thermodynamic properties of the NCAR community climate model, CCM3. *J. Geophys. Res.* **2000**, *105*, (D11), 14873-14890.
42. Hong, S.-Y.; Noh, Y.; Dudhia, J., A new vertical diffusion package with an explicit treatment of entrainment processes. *Mon. Wea. Rev.* **2006**, *134*, (9), 2318-2341.
43. Emmons, L. K.; Walters, S.; Hess, P. G.; Lamarque, J. F.; Pfister, G. G.; Fillmore, D.; Granier, C.; Guenther, A.; Kinnison, D.; Laepple, T.; Orlando, J.; Tie, X.; Tyndall, G.; Wiedinmyer, C.; Baughcum, S. L.; Kloster, S., Description and evaluation of the Model for Ozone and Related chemical Tracers, version 4 (MOZART-4). *Geosci. Model Dev.* **2010**, *3*, (1), 43-67. Parnell, A. C.; Phillips, D. L.; Bearhop, S.; Semmens, B. X.; Ward, E. J.; Moore, J. W.; Jackson, A. L.;
44. Grey, J.; Kelly, D. J.; Inger, R., Bayesian stable isotope mixing models. *Environmetrics* **2013**, *24*, (6), 387-399.
45. Parnell, A. C.; Inger, R.; Bearhop, S.; Jackson, A. L., Source partitioning using stable isotopes: Coping with too much variation. *Plos One* **2010**, *5*, (3), 621-625.
46. Moore, J. W.; Semmens, B. X., Incorporating uncertainty and prior information into



- stable isotope mixing models. *Ecol. Lett.* **2008**, 11, (5), 470-480.
47. Walters, W. W.; Michalski, G., Theoretical calculation of oxygen equilibrium isotope fractionation factors involving various NO<sub>y</sub> molecules, OH, and H<sub>2</sub>O and its implications for isotope variations in atmospheric nitrate. *Geochim. Cosmochim. Ac.* **2016**, 191, 89-101.